Monte Carlo simulations of SEM work with semiconducting devices

E.Napchan, DLM Enterprises, London NW6 1QH, UK
A. Lahav, Technion IIT, Haifa 32000, Israel

Thursday 5th April, 2007 00:42

Contents

List of Tables

List of Figures

1 Introduction

1.1 Monte Carlo simulation

1.1.1 General

1.1.2 Calculation of SE

Two parameters are used in the calculation of the number of secondary electrons emitted from the specimen surface: a generation energy for secondary electrons, and the mean escape depth which affects the number of secondaries that reach the device surface. The number of secondary electrons (generated and emitted) at each primary electron (PE) trajectory step is calculated using the parametric model in [1]:

$$n_{gen} = \frac{\Delta E}{E_{gen}} \tag{1}$$

$$\delta_{emitted} = \frac{n_{gen}\lambda}{z_n - z}\{e^{-z_n/\lambda} - e^{-z/\lambda}\} \tag{2}$$

It is found that the secondary electron mean escape depth is related to the density of defects in the material, and represents the main factor in determining the low energy secondary electron yield [4]. Therefore, this parameter can be used as a fitting parameter when studying films with different characteristics.

1.1.3 Programming the simulation run

The simulation parameters are defined using the following methods, either of the two last used specifying batch simulation parameters:

1. GUI interface where values are entered in 'text boxes'. These values are constant for a specific batch.

2. scanning of a particular variable between a minimum and maximum values, with a specified step. In this way it is possible, for example, to run in one batch simulations for values of beam voltage from 1 to 30, in steps of 0.5.

3. XML file specification of parameters for each run. This is in 'logical' text format, and allows to program a series of simulations to be run as a batch, with as many changes of variables as needed. These variables will take precedence over those declared in method 1 above. An example of an XML file for batch simulation is given in Fig.1.

The advantage of working with XML files are that these are human readable, thus easily prepared, and allow any number of combination of input parameters to be specified for a batch simulation run. In addition, XML is becoming a standard language for information transfer, as it is easily readable and easily parsed by computer programs. Work is currently underway for using XML for all input/output information exchanged with the program, apart from the very large datasets such as the energy deposition matrix.

1.2 Secondary electrons

1.2.1 Experimental data

Experimental data, both for backscattered electrons (BSE) and for secondary electrons (SE) for many materials, extracted from many published sources was collected by D. C. Joy, [9], and is presented in graphical format in the mc-set site [10].

```
<?xml version="1.0" encoding="ISO-8859-1"?>
<PMML version="3.0"
  xmlns="http://www.dmg.org/PMML-3-0"
  xmlns:xsi="http://www.w3.org/2001/XMLSchema_instance" >
  <Header copyright="DLM␣Enterprises">
     Monte Carlo Simulation of Electron Trajectories
     <Application name="mc-set" version="7C16" />
     <XMLDataFile name="mc-set_exp_params.xml" description="Simulation␣parameters␣for␣additional␣C␣SE␣experiments" />
  </Header>
  <SimulationsList>
        <Simulation>
            <DataField name="BeamVoltage" optype="single" dataType="double" value="0.5" units="kVolts" />
            <DataField name="llz" optype="single" dataType="double" value="0.05" units="um" />
        </Simulation>
        <Simulation>
            <DataField name="BeamVoltage" optype="single" dataType="double" value="1" units="kVolts" />
            <DataField name="llz" optype="single" dataType="double" value="0.05" units="um" />
        </Simulation>
        <Simulation>
            <DataField name="BeamVoltage" optype="single" dataType="double" value="1.5" units="kVolts" />
            <DataField name="llz" optype="single" dataType="double" value="0.1" units="um" />
  </SimulationsList>
</PMML>
```

Figure 1: XML batch simulation file

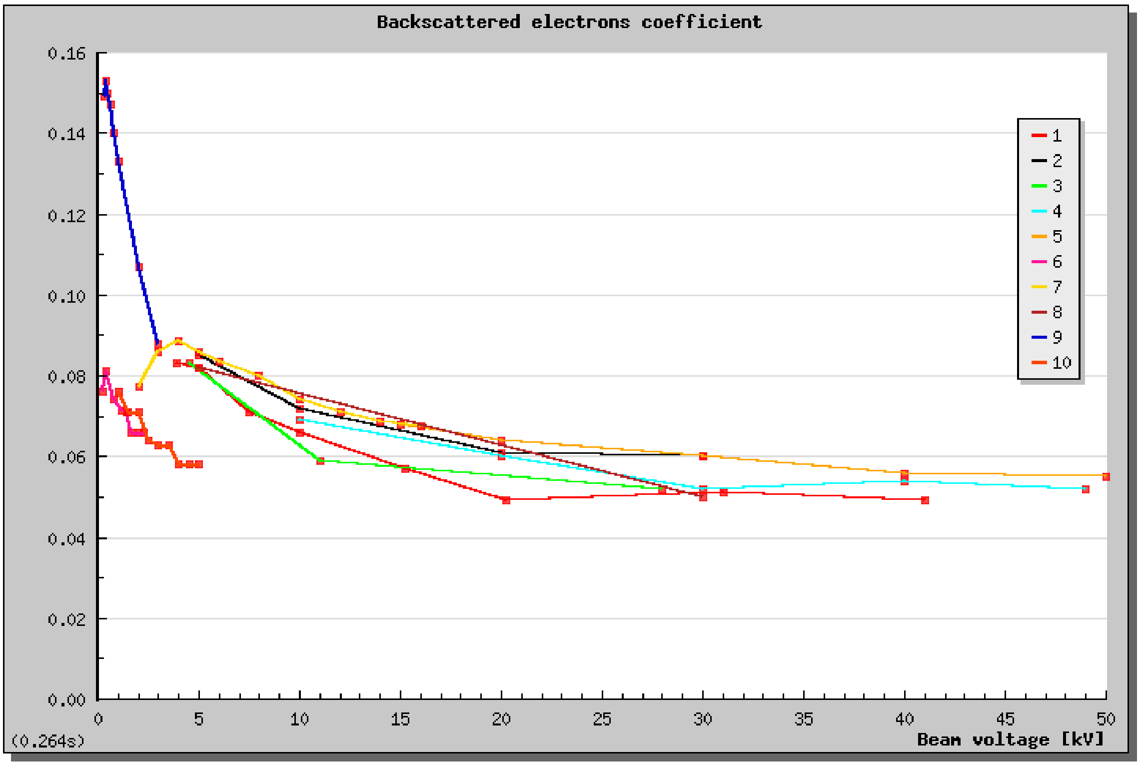

Figure 2: Experimental BSE data for C ([9] in [8])

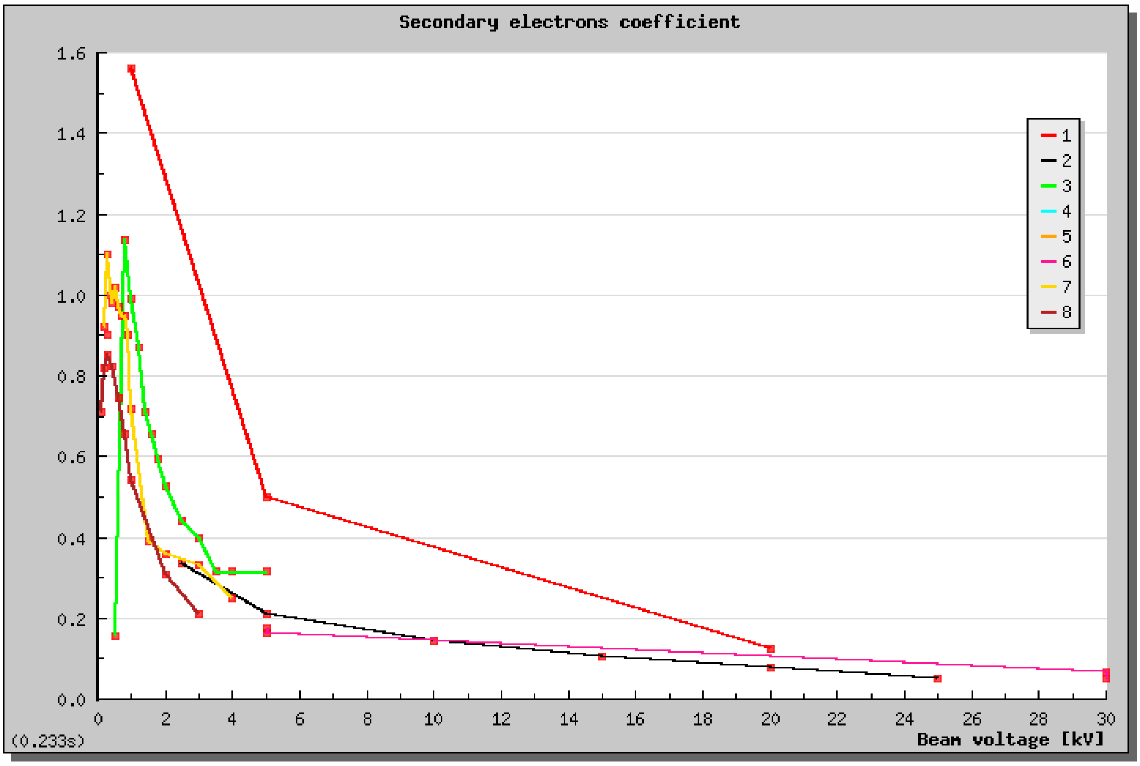

Figure 3: Experimental SE data for C ([9] in [8])

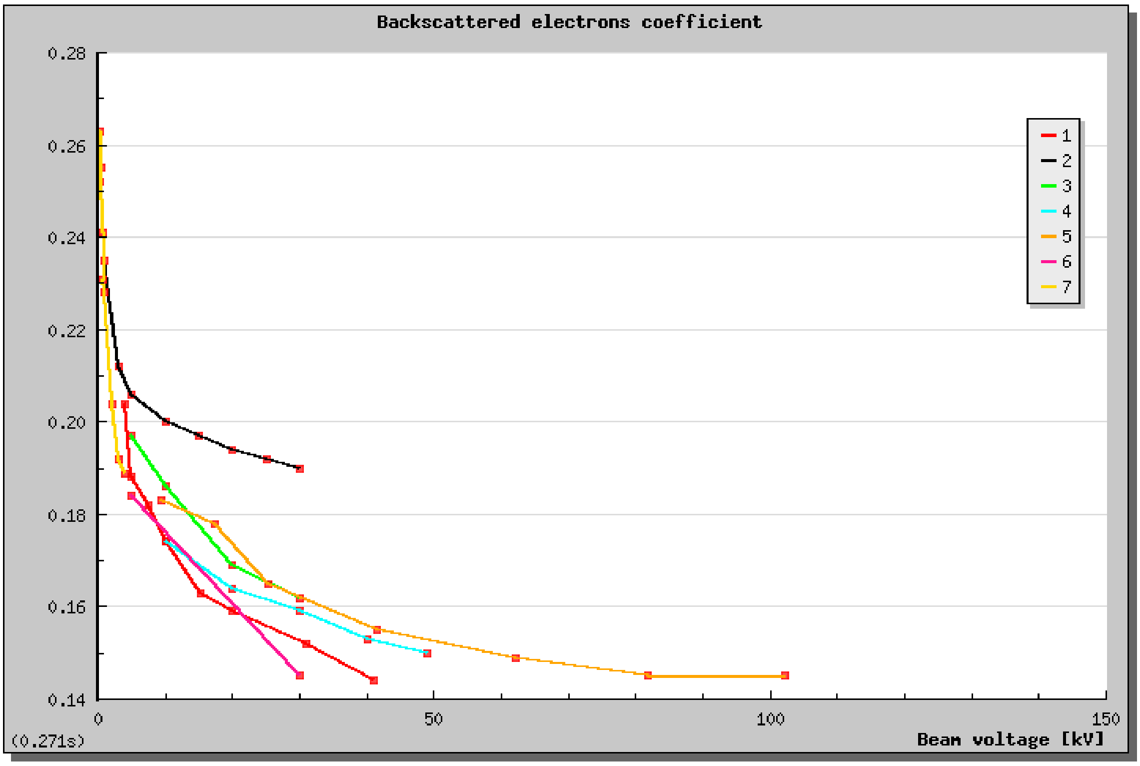

Figure 4: Experimental BSE data for Si ([9] in [8])

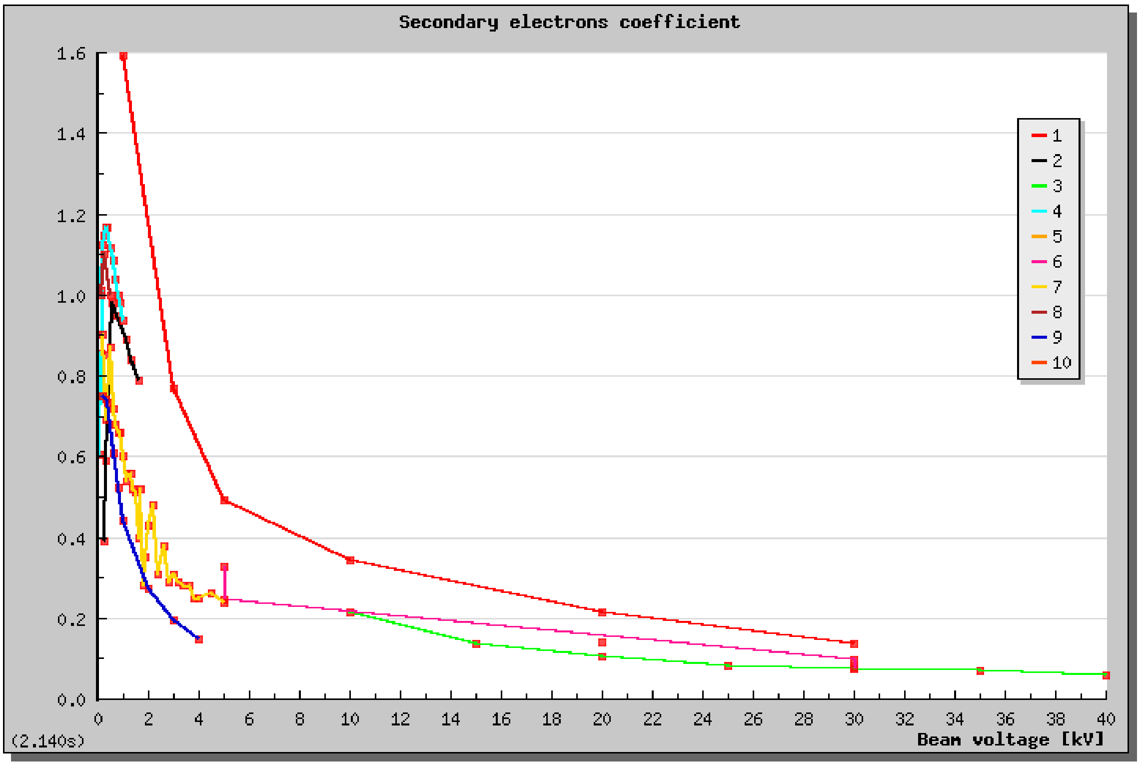

Figure 5: Experimental SE data for Si ([9] in [8])

Fig. 1.2.1 and Fig. 1.2.1 presents BSE and SE experimental data available in these sources for Carbon. Fig. 1.2.1 and Fig. 1.2.1 present the corresponding data for Silicon.

One suggested explanation, [6], for the spread in the experimental results is the state of the device surface. For Carbon, there is a large variation between cleaned/uncleaned sample and also between other experimental results for the backscattered electron coefficient.

It seems natural that the spreads in results will also affect secondary electrons due to their lower generation depth, and therefore, their higher sensitivity to surface conditions. The effect is expected to be stronger for lower beam voltages and for low atomic number specimens, as shown in [6].

1.2.2 Comparison with MC–SET results

- Silicon dioxide SE and BSE experimental values for SiO2 from the database are compared with those calculated using the simulation. Fig.1.2.2 shows the single available experimental data in the database, which is compared with results from the Monte Carlo simulation using two different sets of parameters for the material parameters: 2.5, 123.00 and 234.00 for the top curve, and 2.2, 10.8 and 21.6 for the lower curve.

  It is clearly seen that the “correct” values for the material parameters give a better fit to the experimental BSE data.

  The SE calculated data was evaluated using the parameters in [1], for both sets of material parameters used. With an adjustment of the energy required to create an SE, from 40 eV to 50 eV, and to 60 eV, for the two sets of data it was possible to obtain a good fit between the simulated data and the experimental SE data. Fig.1.2.2 and Fig.1.2.2 show the SE yield for both sets of material parameters, as given above.

- Silicon

- Gallium Arsenide

- Carbon

Experimental and simulated results for secondary electron and backscattered electron yields for Carbon are given in [3], Fig. 4. These are compared with simulated results obtained using MC–SET.

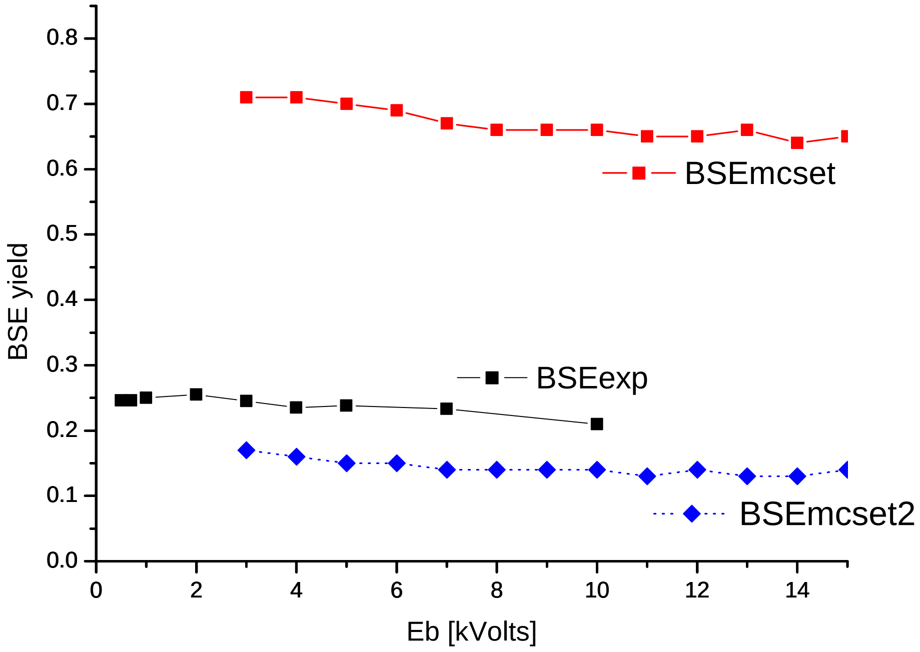

Figure 6: BSE yield for Silicon Dioxide: experimental and simulations

Another source of experimental data compared to data calculated using an old version of MC–SET aappears in [5]. Here both the secondary and backscattered electron yields were measured, and the simulation results adjusted to get a best fit.

Further results of backscattering coefficient values calculated by Monte Carlo methods and their fit to experimental data (same experimental data as in [3]) is presented in [7].

1.2.3 Platinum

Experimental and simulated results for secondary electron and backscattered electron yields for Carbon are given in [3], Fig. 3. These are compared with simulated results obtained using MC–SET.

2 Focussed Ion Beam work

Dual beam systems, combining a Focussed Ion Beam (FIB) for specimen thinning by milling, with a Scanning Electron Microscope (SEM) for real time observation, have become a standard tool for nanofabrication and for Transmission Electron Microscopy (TEM) sample preparation ([11], [12] and [13]). The target thickness of TEM samples is typically 50 to 200 nm, depending on material and required TEM resolution.

A FEI Company Strata 400 Dual Beam FIB/STEM System was used for thin sample preparation and SE contrast measurements. The FIB column, with Ga liquid metal ion source, was operated at 2 - 30 kVolts and current between 1 pA and 21 nA. The SEM column, with Schottky field emission source, allowed operation in 1 30 kVolts range. Secondary electron detection for imaging is carried out with an Everhart Thornley (ETD) and a Thru-the-Lens similar (TLD) detector. In addition, the system has Scanning Transmission Electron Microscopy (STEM) detectors.

The Everhart Thornley Detector (ETD), a scintillator/photo-multiplier type detector is mounted above and to one side of the sample, and is operated with grid voltages of +250 Volts for secondary electron collection, and -150 Volts for backscatter electron collection. The TLD SE detector is of a similar type detecto,r located inside the SEM lens, directly above the sample.

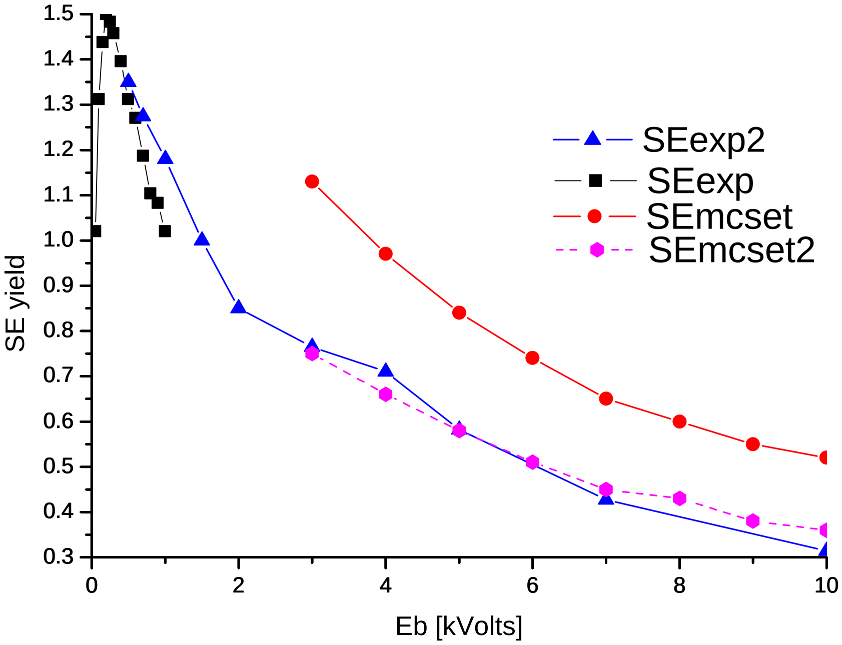

Figure 7: SE yield for Silicon Dioxide: experimental and simulations (bad material parameters) [ht]

2.1 Sample preparation

A Silicon on Insulator (SOI) sandwich (Si 2 micron / SiO2 1.9 micron / bulk Si substrate (001) orientation) and a GaAs (001) wafer were used for thin samples preparation. First, a layer of Platinum (about 2 μm) was deposited by FIB to protect the top surface during sample thinning. Thin cross–sections (about 1 mum thick), for both Si and GaAs, were milled using the FIB normally to the sample surface. They were than lifted out using an Omniprobe micromanipulator, and attached to a TEM grid on the Flip Stage.

The cross-sections were further thinned on the Flip Stage with FIB at 30KeV and current ranging from 460 to 100 pA at a glancing angle of 1 degree from both sides. One side of the samples was cut flat, while the other side was cut in the form of steps of different thickness.

Fig.9(a) shows a side view of the Si sample oriented normally to PE beam, with the flat side facing the electron column. The sample has 10 steps (segments) of different thickness, their width between 3 to 1.5 microns. Fig..9(b) shows a top view of the sample. The thinnest segment no. 20 has developed a hole in the bottom part and has bowed in its top part.

The GaAs sample is shown in Fig.10 in similar orientation. This specimen had 13 steps. It can be seen that for the segments 9 -13 the Pt protection layer has been completely removed, and that the top portion of the sample has been milled away.

2.2 Experimental observations

It was experimentally observed that for a selected SEM voltage, the SE contrast measured by the detector located at the sample side, starts to increase during sample milling, as the sample becomes transparent for the PE beam.

With further specimen thinning, the SE contrast reaches a maximum, after which it starts to decrease.

This contrast variation of the SE signal is only observed with the side ETD, which suggested the additional source of secondary electrons as coming from the bottom surface of the device. Fig.11 a) and b) shows images obtained with the two types of SE detectors described. It is clearly seen from these images that the SE intensity goes through a maximum value for the ETD detector, while the change in SE signal for the TLD does not show such behaviour.

The thicknesses of each segment in both samples described above were measured in top view using High Resolution SEM, and are given in Table2.2. The Silicon specimen was measured in the SEM after

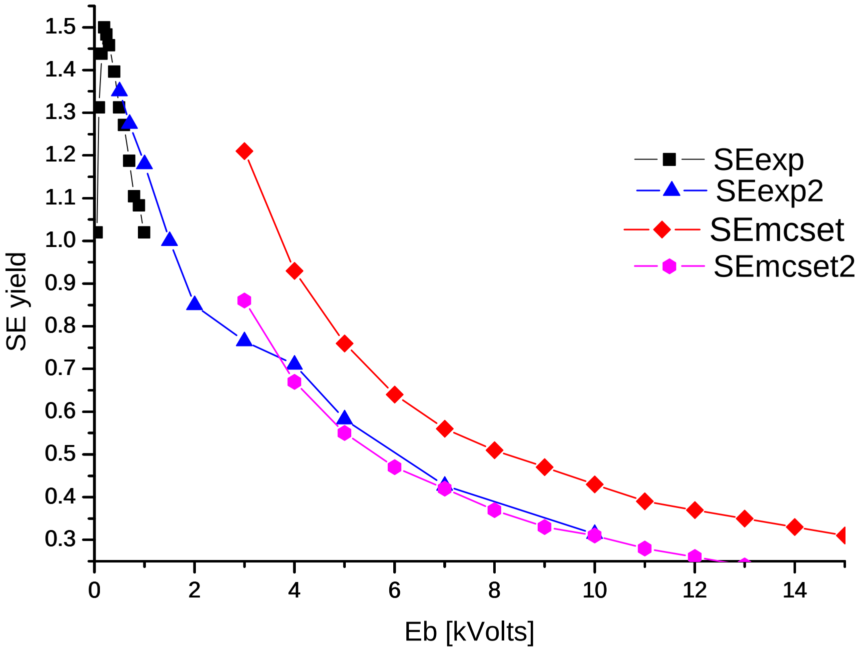

Figure 8: SE yield for Silicon Dioxide: experimental and simulations

the first thinning, then it was thinned again and further measurements were taken.

Si (1) [idx]	Thick. [nm]	Si (2) [idx]	Thick. [nm]	GaAs [idx]	Thick. [nm]
1	1330	11	890	1	640
2	1050	12	620	2	535
3	850	13	560	3	450
4	620	14	500	4	410
5	510	15	350	5	375
6	390	16	270	6	315
7	300	17	240	7	260
8	210	18	180	8	200
9.1	160	19	100	9	150
9.2	145	20	75	10	115
9.3	115			11	90
				12	70
				13	50

Table 1: Thicknesses of GaAs and Si specimens (the index for the various segments appear in the corresponding SE images)

3 Discussion

3.1 Simulation

The comparison of simulated results with those available in the summary of literature values, as given in the electrons scattering parameters database in [8] is an important tool for checking the simulation results obtained. In the case of Silicon Dioxide it was found that disparate material parameters would result in “good” SE yield results for a range of accelerating voltages, after adjusting one of the parameters used for SE calculations. When the “correct” values were used, a better fit, both to the SE and to the BSE experimental results, was obtained.

This checking needs to cover as many calculated parameters as feasible, and needs to be done whenever changes, either in simulation methods, or material properties are introduced.

3.2 SE signal variation as function of thickness

For the SE yield as a function of specimen thickness (both for the Monte Carlo simulations and for the experimental work), it is possible to distinguish singular points in the yield curves, as function of the beam accelerating voltage:

- for the simulations: the beginning of contrast increase when primary electrons start exiting the specimen from its bottom surface, and when trajectory steps occur near this second surface
- for the experimental work: a relative value for SE intensity is assigned: 1 for maximum brightness, 0 for darkness, and 0.2 for "image becoming britgher"

The contrast change points as defined above, in particular those based on the experimental results, can be used to construct tables for materials processing. These tables will specify the thickness of the layer when the contrast starts to change, for a particular beam voltage.

3.3 Silicon Dioxide results

A graph of some experimental results for 15, 10 and 5 kVolts for SiO2 is shown in Fig.12.

3.4 Silicon results

The following Fig.13 shows the observed experimental relative values for the SE intensity for the various segments at the beam accelerating voltages used. These include both stages of thinning in this specimen.

Fig. 14 and 15 give the simulated SE yields for Silicon under varying conditions of beam voltage and thickness.

3.5 Gallium Arsenide results

The following Fig.16 shows the experimental relative values for the SE intensity for the various segments at the beam accelerating voltages used.

Fig. 17 and 18 give the simulated SE yields for GaAs under varying conditions of beam voltage and thickness.

3.6 Other materials

Simulations and experimental SEM work were also carried out for other materials, as device layers, with the same SE behaviour observed. Fig. 19 and Fig. 20 show some of the results obtained for Gold and for Silicon Nitride, commonly used as device layers.

3.7 Comparison between experiment and simulation

The simulation results obtained are fully quantitative in that the links between the SE yield and the primary beam electrons are linked via the simulation methods and parameters used. The final qualitative product of the simulation was a graph of SE yield as function of beam voltage, for a particular thickness of the selected material.

The next stage in the use of this data brings a certain measure of uncertainty: the position along the curve where the signal starts to increase, and the position of the maximum SE value have to be estimated for a particular beam voltage. From this position, a specific material thickness is derived.

The experimental SE data is even more quantitative. The SE values at each device segment were digitized (in a selected area for averaging), and these were plotted graphically as function of beam voltage and segment thickness. Using the original image and this plot, the maximum SE position was estimated, along with the position when the SE contrast starts changing for a particular segment. The results were material thickness for each condition, as a function of beam voltage.

The two sets of estimated data, from the simulation and from the experimental images, for the conditions of SE maximum and SE just starting to increase were then plotted and compared. Figs. 21 and 22 shows this comparison, for Silicon and for GaAs, respectively.

4 Conclusion and further work

4.1 Experimental

The results in this paper allow an estimate of the thickness of devices during FIB fabrication based on the observed secondary electron images. The device thickness during processing can be estimated by noting the start of increase in SE yield, and by observing the maximum value of this signal.

The experimental results were analysed using Monte Carlo simulations of electron trajectories, and equivalent data was compared. For both materials studied, Silicon and Gallium Arsenide, the experimental results were in agreement with those from the simulation, in particular for the GaAs.

Further experiment related work:

- **SE signal from both layers** It should be bourne in mind that the issues discussed in this paper are only applicable when the electrons emitted from the bottom surface of the device under observation can contribute to the overall secondary electron signal. Further work is under way to understand contrast variations when only the top layer secondary electron signal is measured.

- **Better quantitative SE measuremnts** Most of the measurements of SE signal in this work were carried out by digitizing (and averaging) values from the recorded micrographs. Settings of the SE detector where not changed between different measurements, and therefore the images could be compared. It would be useful to have an absolute scale for SE signal, which would take into consideration the detector settings, allowing a direct comparison betwen different measurements.

4.2 Simulation

Further simulation work:

- **Use of energy matrix** It was possible to calculate the SE signal by using the stored energy matrix for a simulation. This allowed easily varying the SE generation and absorption parameters, without the need to rerun the simulation. More checks should be made for the accuracy of the results obtained using the matrix.

- **Data compression** The large number of simulations carried out for which the energy matrix deposition was saved needed a large amount of disk space: partial results occupied almost 5 gigabytes of data, making its transfer and management a difficult task. Further modifications to the simulation program will include ways of reducing the storage required for enery data, along with better ways to manage large data sets comprising of a number of simulations.

- **Different models for the SE electron generation** to be used in the simulation, which perhaps will yield different results. Examples of such models (described in [1]) are the first principles SE generation, and the fast secondary model.

- **Standard input/output language** XML to be used for all data transfer in the simulation. Allow the GUI screen to display the XML file data. Use XML (and perhaps Excel format) to export data from the BSE graphical database of electron scattering data.

References

[1] *Monte Carlo Modeling for Electron Microscopy and Microanalysis*; D. C. Joy; Oxford University press (1995)

[2] *Scanning Electron Microscopy - Physics of Image Formation and Microanalysis*, Second Edition; L. Reimer; Springer Series in Optical Sciences Volume 45 (1998)

[3] Monte Carlo simulation of secondary electron and backscattered electron images for a nanoparticle-matrix system, Y T Yue, H M Li and Z J Ding, J. Phys. D: Appl. Phys. 38 (2005) 1966–1977

[4] Secondary electron emission from diamond: Physical modeling and application to scanning electron microscopy, P Ascarelli et. al., J. Appl. Phys., Vol. 89, No. 1, 1 January 2001

[5] Farhang H. et al. Electron backscattering and secondary electron emission from carbon targets: comparison of experimental results with Monte Carlo simulations, J. Phys. D: Appl. Phys. 26, pp. 2266-2271, 1993

[6] Backscattering coefficients for low energy electrons, A.M.D. Assa'd and M. M. El Gomati, Scanning Microscopy Vol. 12, No. 1, 1998 (Pages 185-192)

[7] Fitting a simple model of inelastic scattering in Monte Carlo code to experimental data, V Stary, J. Phys. D: Appl. Phys. 32 (1999) 18111818

[8] Database of bacscattered and secondary electron experimental data, *http://www.mc-set.com*, Graphic presentation of DC Joy database (2006)

[9] *A Database of Electron-Solid Interactions - Revision 04-02*, The complete database, containing tabulations of all available data sets as well as a comprehensive bibliography, can be downloaded as a Microsoft Word document from http://web.utk.edu/ srcutk/htm/interact.htm (2006)

[10] MC–SET ,*http://www.mc-set.com* (free download), Monte Carlo Simulation of Electron Trajectories (2007)

[11] Robert Krueger, Dual-column (FIBSEM) wafer applications, Micron 30 (1999) 221226

[12] V. G. M. Sivel , et al., Application of the dual-beam FIB/SEM to metals research, Journal of Microscopy, Vol. 214, Pt 3 June 2004, pp. 237245

[13] Steve Reyntjens and Robert Puers, A review of focused ion beam applications in microsystem technology", Journal of Micromechanics and Microengineering, 11 (2001) 287300

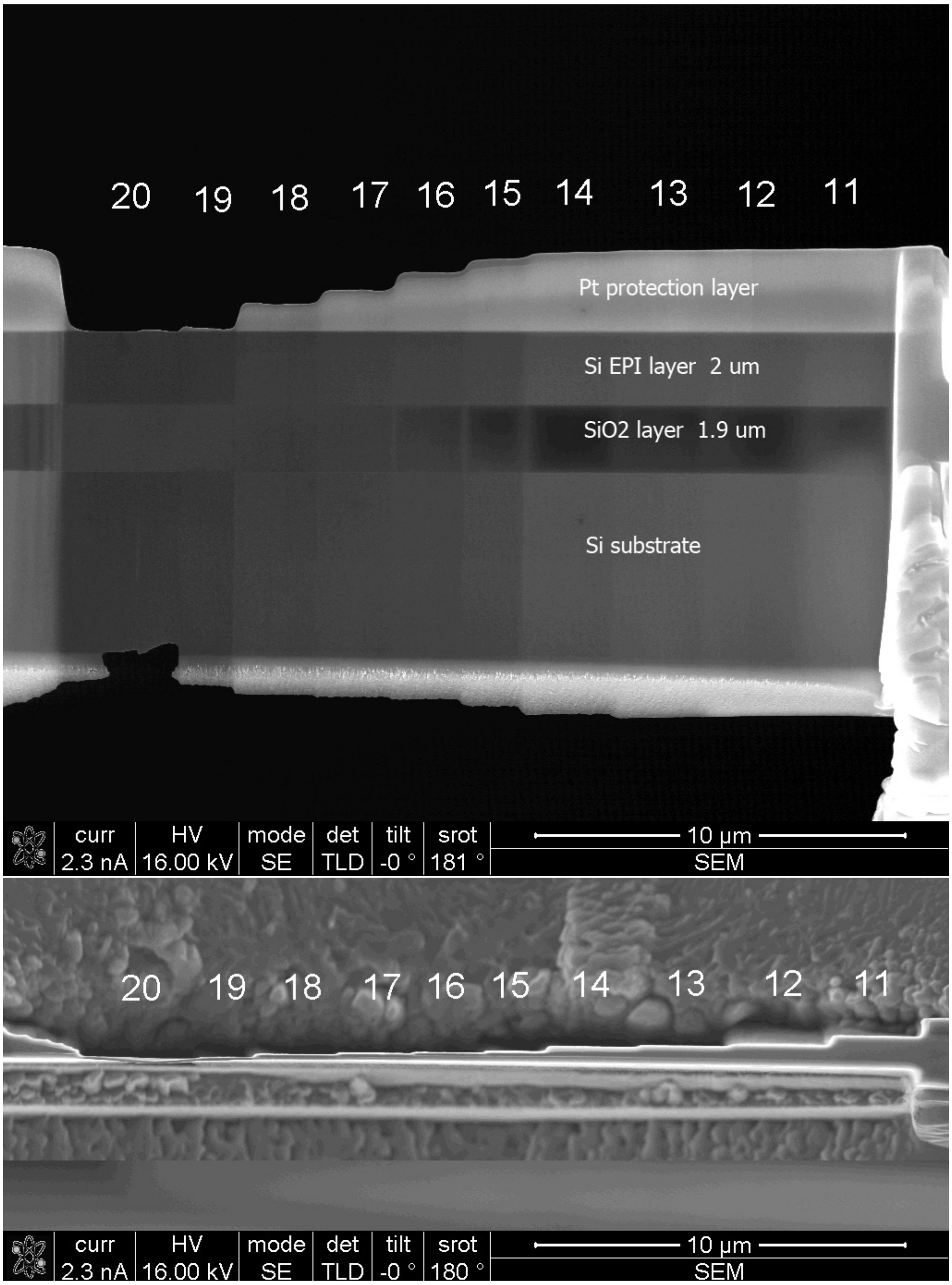

Figure 9: SE images of the SOI specimen (top and side)

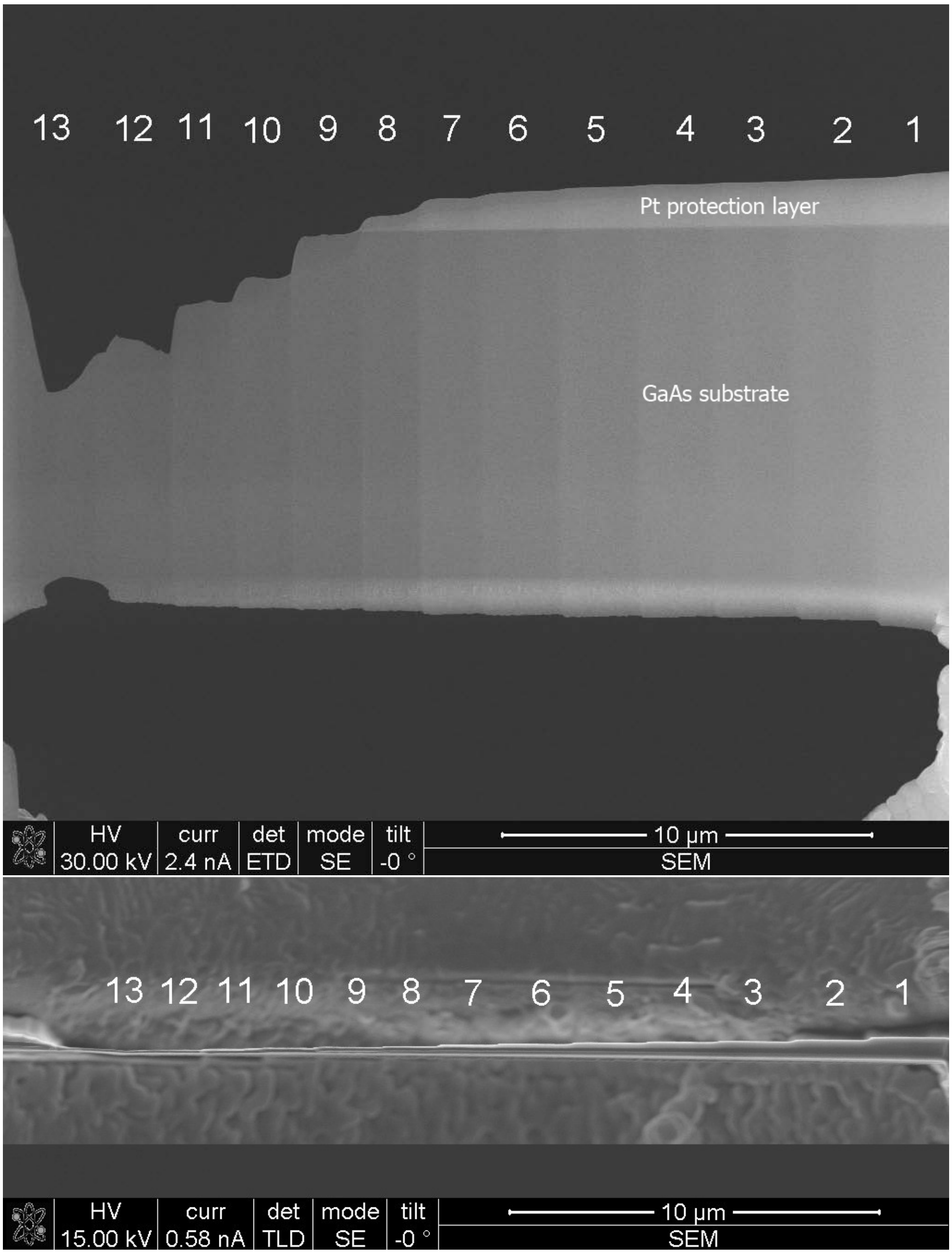

Figure 10: SE images of the GaAs specimen (top and side)

Figure 11: SE images from different detectors

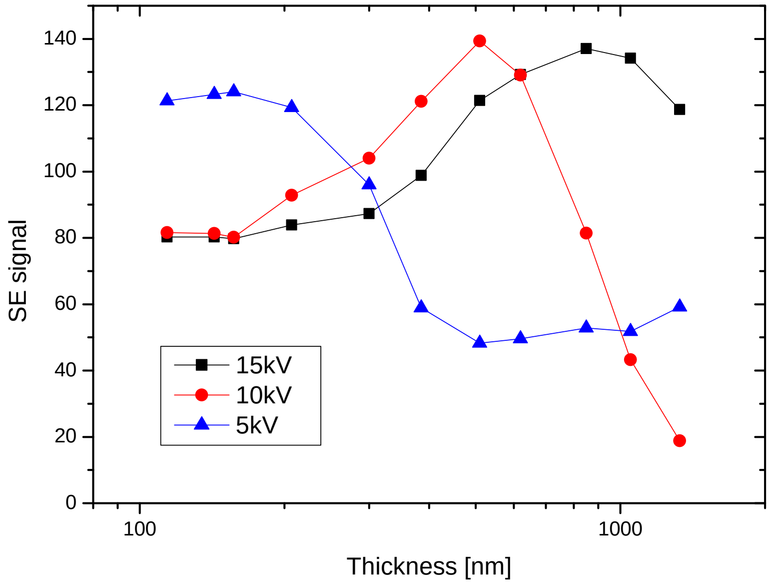

Figure 12: SE experimental data for SiO2 as function of sample thickness for 3 beam voltages

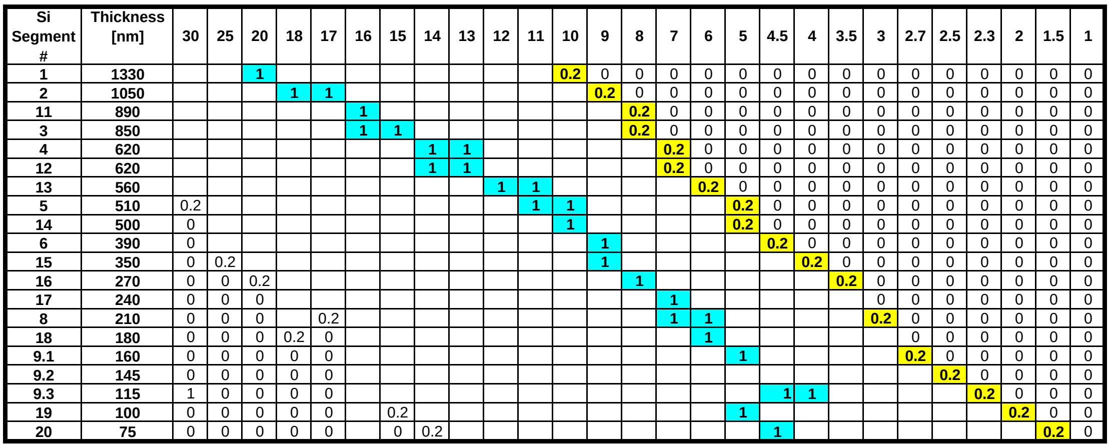

Si Segment #	Thickness [nm]	30	25	20	18	17	16	15	14	13	12	11	10	9	8	7	6	5	4.5	4	3.5	3	2.7	2.5	2.3	2	1.5	1
1	**1330**			**1**									**0.2**	0	0	0	0	0	0	0	0	0	0	0	0	0	0	0
2	**1050**				**1**	**1**								**0.2**	0	0	0	0	0	0	0	0	0	0	0	0	0	0
11	**890**						**1**								**0.2**	0	0	0	0	0	0	0	0	0	0	0	0	0
3	**850**						**1**	**1**							**0.2**	0	0	0	0	0	0	0	0	0	0	0	0	0
4	**620**								**1**	**1**						**0.2**	0	0	0	0	0	0	0	0	0	0	0	0
12	**620**								**1**	**1**						**0.2**	0	0	0	0	0	0	0	0	0	0	0	0
13	**560**										**1**	**1**					**0.2**	0	0	0	0	0	0	0	0	0	0	0
5	**510**	0.2										**1**	**1**					**0.2**	0	0	0	0	0	0	0	0	0	0
14	**500**	0											**1**					**0.2**	0	0	0	0	0	0	0	0	0	0
6	**390**	0												**1**					**0.2**	0	0	0	0	0	0	0	0	0
15	**350**	0	0.2											**1**						**0.2**	0	0	0	0	0	0	0	0
16	**270**	0	0	0.2											**1**						**0.2**	0	0	0	0	0	0	0
17	**240**	0	0	0												**1**						0	0	0	0	0	0	0
8	**210**	0	0	0		0.2										**1**	**1**					**0.2**	0	0	0	0	0	0
18	**180**	0	0	0	0.2	0											**1**						0	0	0	0	0	0
9.1	**160**	0	0	0	0	0												**1**					**0.2**	0	0	0	0	0
9.2	**145**	0	0	0	0	0																		**0.2**	0	0	0	0
9.3	**115**	1	0	0	0	0													**1**	**1**					**0.2**	0	0	0
19	**100**	0	0	0	0	0		0.2										**1**								**0.2**	0	0
20	**75**	0	0	0	0	0		0	0.2										**1**								**0.2**	0

Figure 13: SE experimental data for Si: relative values, for beam voltages between 30 and 1 kVolts (see text for explanation about values)

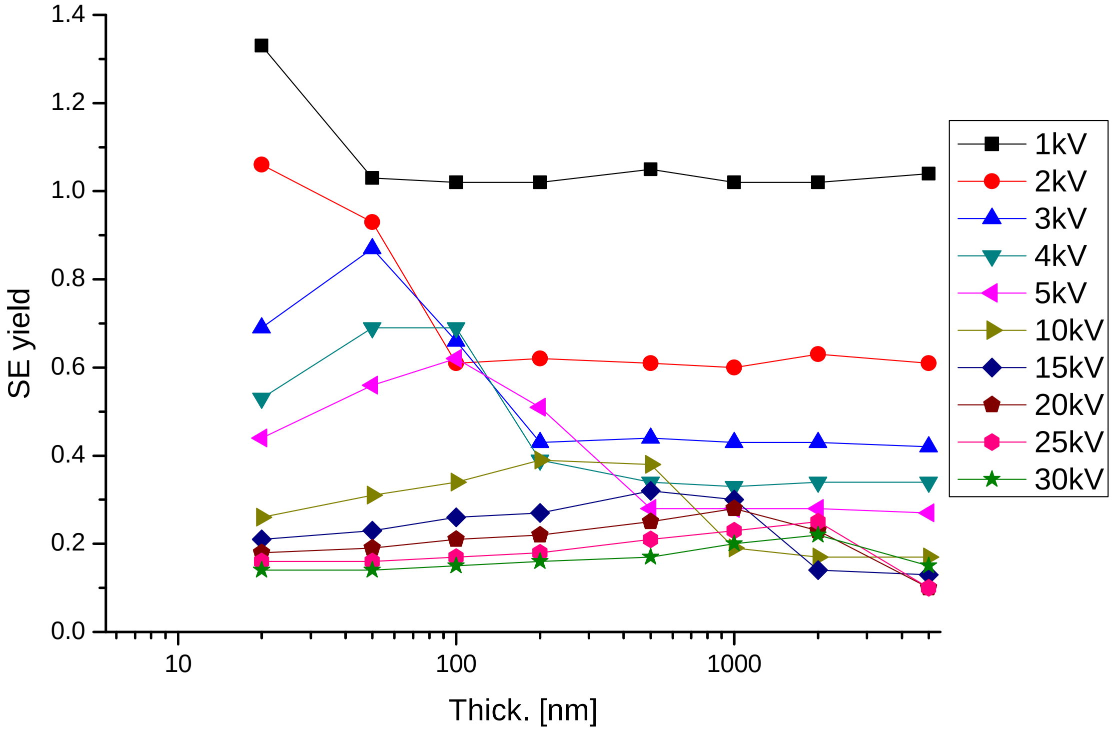

Figure 14: Simulated SE yield for Si, for beam voltages between 1 and 30 kVolts

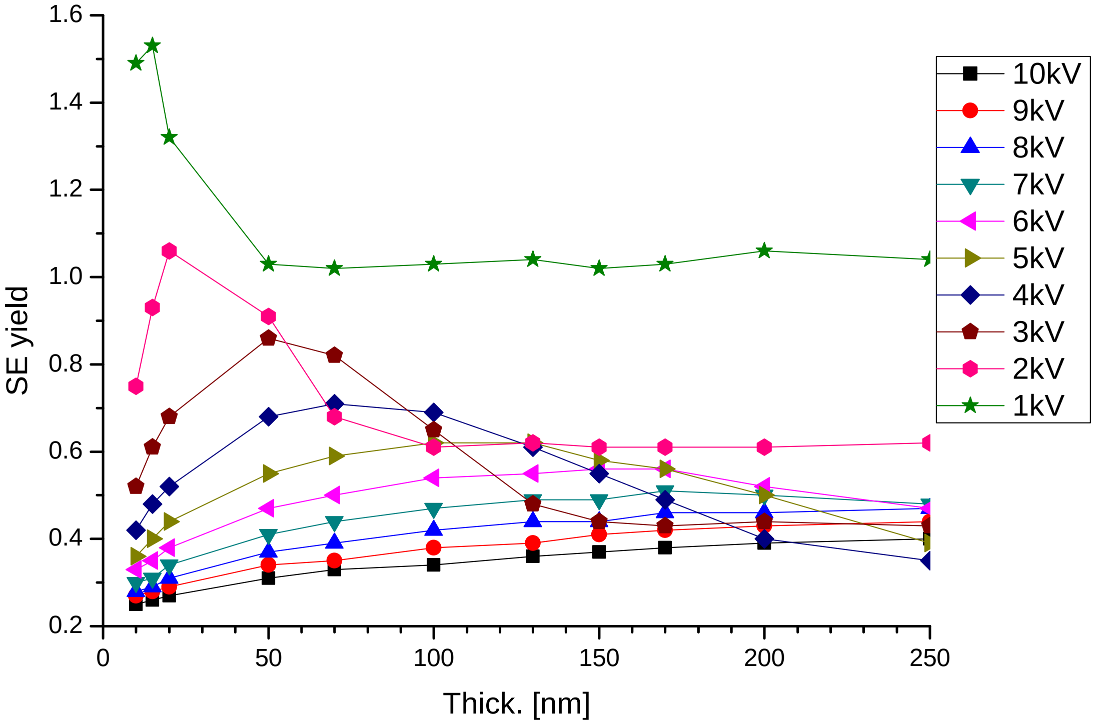

Figure 15: Simulated SE yield for Si: for beam voltages between 1 and 10 kVolts

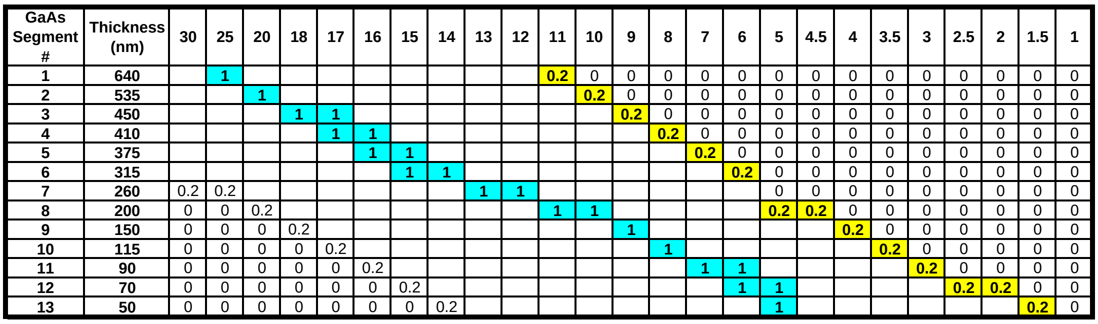

GaAs Segment #	Thickness (nm)	30	25	20	18	17	16	15	14	13	12	11	10	9	8	7	6	5	4.5	4	3.5	3	2.5	2	1.5	1
1	640		1									0.2	0	0	0	0	0	0	0	0	0	0	0	0	0	0
2	535			1									0.2	0	0	0	0	0	0	0	0	0	0	0	0	0
3	450				1	1								0.2	0	0	0	0	0	0	0	0	0	0	0	0
4	410					1	1								0.2	0	0	0	0	0	0	0	0	0	0	0
5	375						1	1								0.2	0	0	0	0	0	0	0	0	0	0
6	315							1	1								0.2	0	0	0	0	0	0	0	0	0
7	260	0.2	0.2							1	1							0	0	0	0	0	0	0	0	0
8	200	0	0	0.2								1	1					0.2	0.2	0	0	0	0	0	0	0
9	150	0	0	0	0.2									1						0.2	0	0	0	0	0	0
10	115	0	0	0	0	0.2									1						0.2	0	0	0	0	0
11	90	0	0	0	0	0	0.2									1	1					0.2	0	0	0	0
12	70	0	0	0	0	0	0	0.2									1	1					0.2	0.2	0	0
13	50	0	0	0	0	0	0	0	0.2									1							0.2	0

Figure 16: SE experimental data for GaAs: relative values, for beam voltages between 30 and 1 kVolts (see text for explanation about values)

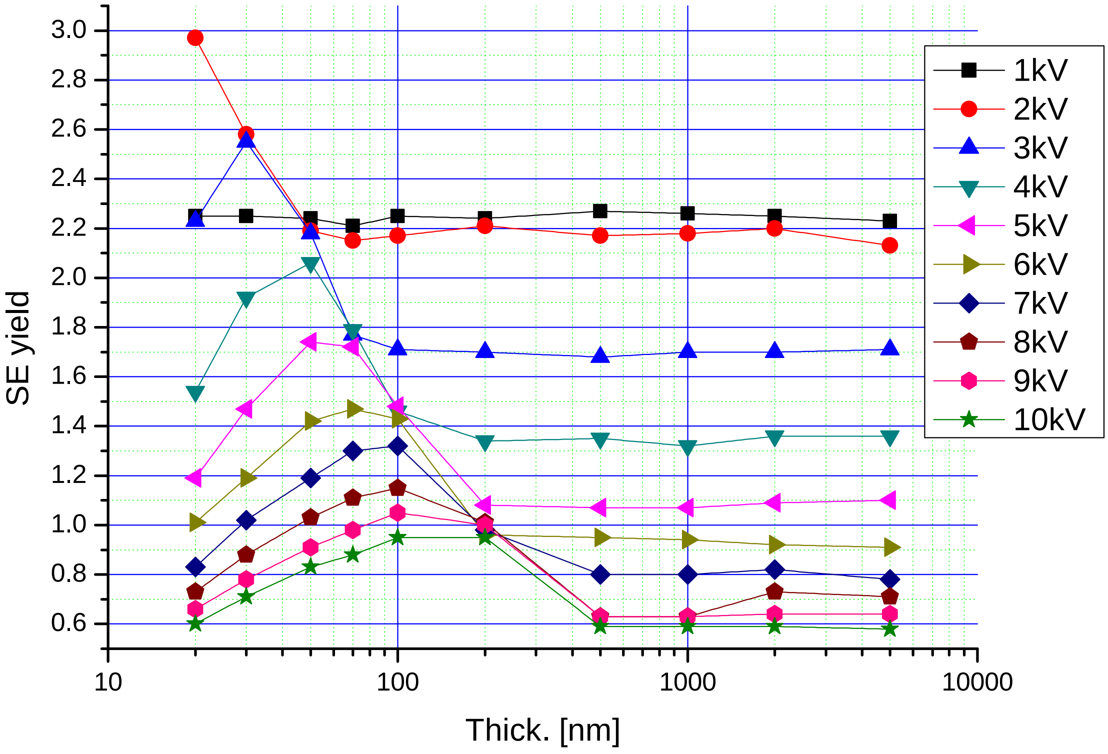

Figure 17: Simulated SE yield for GaAs: for beam voltages between 1 and 10 kVolts

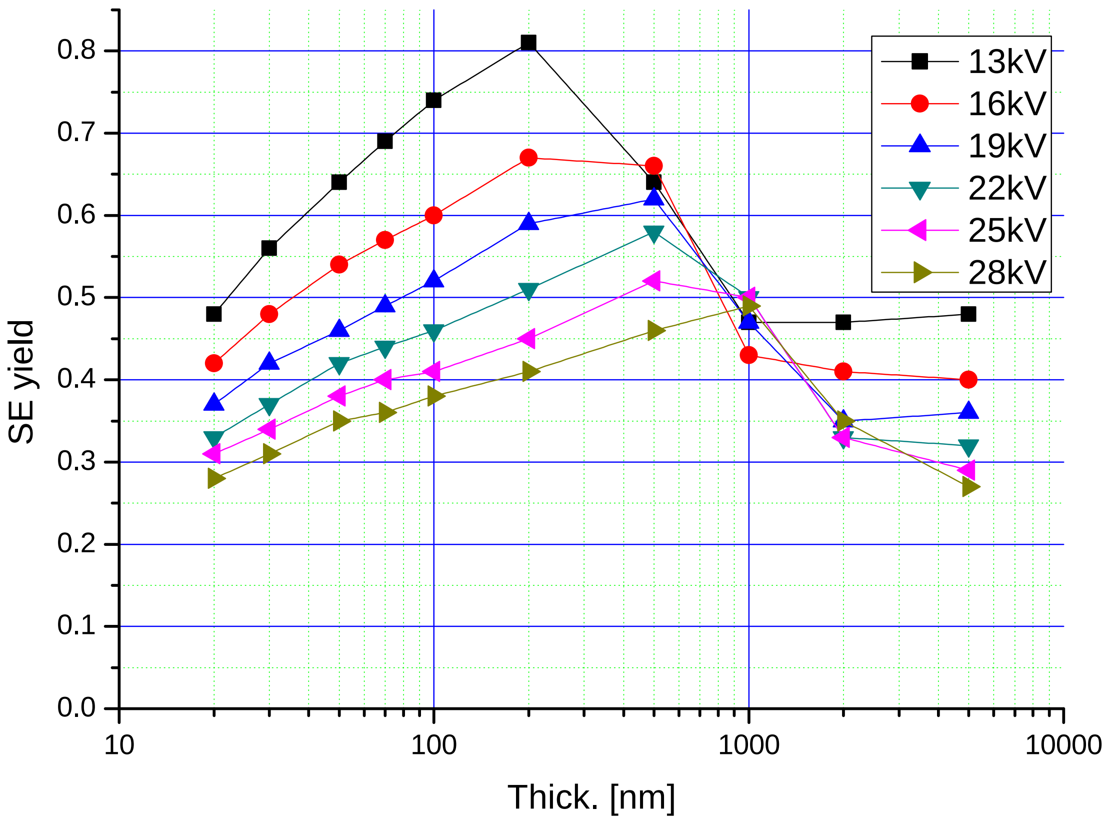

Figure 18: Simulated SE yield for GaAs: for beam voltages between 13 and 30 kVolts

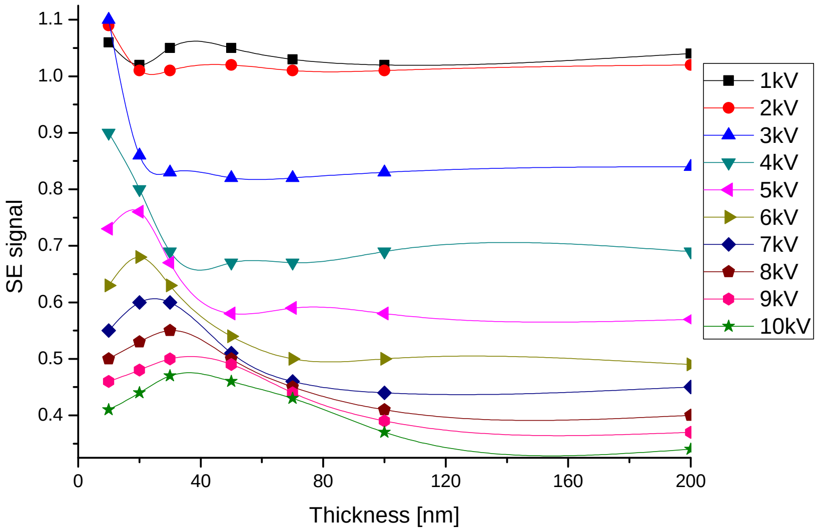

Figure 19: Simulated SE signal for Gold thin films

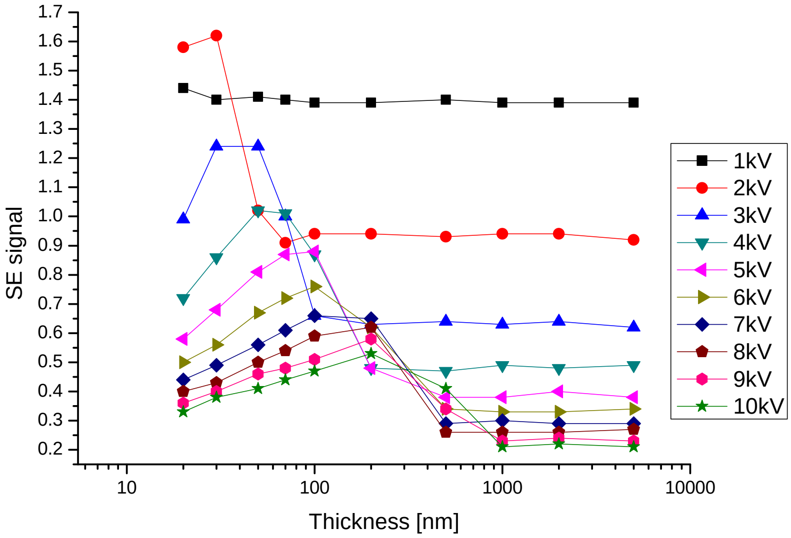

Figure 20: Simulated SE signal for Silicon Nitride thin films

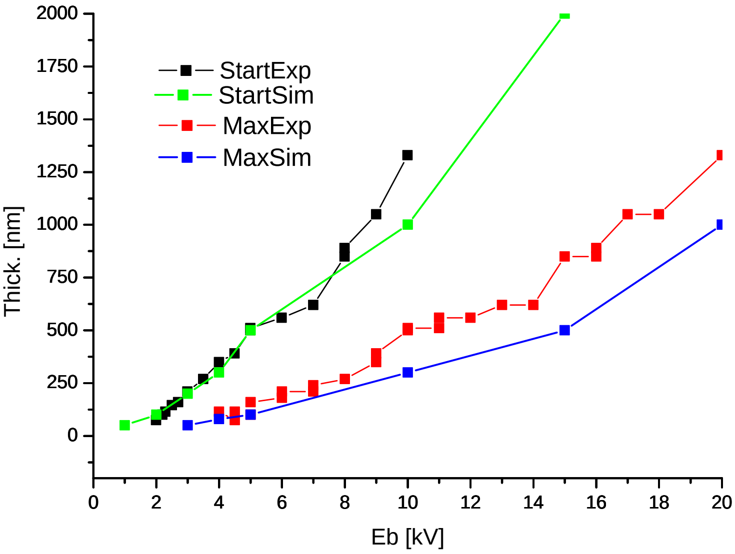

Figure 21: Comparison between experimental and simulated SE yield for Silicon as function of beam voltage and specimen thickness, for both SE variation positions: start of change and maximum SE value

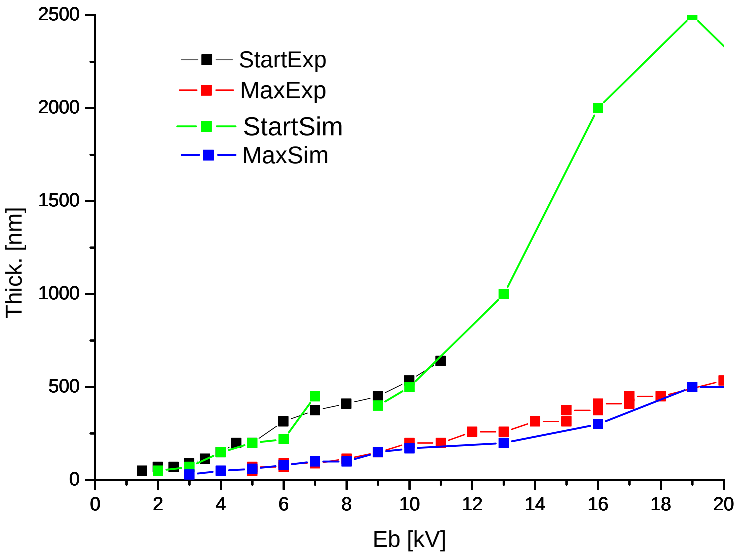

Figure 22: Comparison between experimental and simulated SE yield for GaAs as function of beam voltage and specimen thickness, for both SE variation positions: start of change and maximum SE value